AGU100 ADVANCING EARTH AND SPACE SCIENCE

Geochemistry, Geophysics, Geosystems

RESEARCH ARTICLE
10.1029/2017GC007354

Special Section:
Magnetism in the Geosciences – Advances and Perspectives

Thermoremanent Behavior in Synthetic Samples Containing Natural Oxyexsolved Titanomagnetite

Emma Hodgson[1], J. Michael Grappone[1], Andrew J. Biggin[1], Mimi J. Hill[1], and Mark J. Dekkers[2]

[1]Geomagnetism Laboratory, School of Environmental Sciences, University of Liverpool, Liverpool, UK, [2]Paleomagnetic Laboratory Fort Hoofddijk, Utrecht University, CD Utrecht, The Netherlands

Key Points:
- Artificial specimens are subjected to thermoremanent behavior tests
- Oxyexsolved titanomagnetite grains behave similarly to multidomain grains in paleointensity experiments
- Increasing the temperature of the initial step in the experiment decreased the observed curvature in the Arai plot

Correspondence to:
J. M. Grappone,
grappone@liv.ac.uk

Citation:
Hodgson, E., Grappone, J. M., Biggin, A. J., Hill, M. J., & Dekkers, M. J. (2018). Thermoremanent behavior in synthetic samples containing natural oxyexsolved titanomagnetite. *Geochemistry, Geophysics, Geosystems*, *19*, 1751–1766. https://doi.org/10.1029/2017GC007354

Received 30 NOV 2017
Accepted 26 APR 2018
Accepted article online 8 MAY 2018
Published online 22 JUN 2018

Abstract Understanding Earth's geodynamo provides us a window into the evolution of the Earth's core, which requires accurate data about how its strength varies with time. Classic Thellier-style paleointensity experiments assume that studied specimens contain only noninteracting single-domain (SD) magnetic particles. Interacting grains commonly occur in volcanic rocks but are generally assumed to behave like equivalently sized SD grains. Multidomain (MD) grains can cause erroneous PI estimates or cause Thellier-style experiments to fail entirely. Synthetic specimens containing naturally formed magnetite with MD grains and oxyexsolved titanomagnetite (closely packed SD grains) were subjected to various partial thermoremanent magnetization (pTRM) experiments, which tested nonideal behavior as a function of pTRM acquisition and loss inequality, thermal history, and repeated heating steps. For all grain sizes and domain states, pTRMc (heating and cooling in a nonzero field) gives larger values, compared to pTRMb (heating in a zero field and cooling in a nonzero field), by ~5.5%. Oxyexsolved grains appear prone to the same concave-up, nonideal Arai plots commonly observed in MD specimens, which also has potential implications for the multiple-specimen, domain-state corrected protocol. Repeated heatings cause additive deviations from ideality with relatively small impacts on Arai plot curvature for both grain types. Experiments with higher initial demagnetization temperatures had lower curvatures, with the most SD-like behavior occurring in the uppermost 20°C of the (un)blocking temperature range. Samples containing mixtures of magnetic domain sizes are likely to behave less ideally at lower temperatures but become more ideal with increasing temperature as the nonideal grains unblock.

Plain Language Summary The strength of the magnetic field of the Earth is controlled by changes deep in the Earth. Studying the magnetization of ancient lava flows helps us determine the history of these changes because lavas become magnetized when they cool in the Earth's magnetic field. In this paper, we used artificial rocks to study how changing the size of and distance between the magnetic particles inside the rocks affects how we can determine the past strength of Earth's magnetic field. We found that both larger particles and more closely packed particles cause our estimates for the magnetic field strength to be too high. We also found that heating the rock samples to the same temperature multiple times causes their magnetization to change each time (for rocks with small, far-apart particles, only the first heating changes the magnetization). For future studies, steps must be taken to ensure that the nature of the magnetic particles in the rocks is known and that they are suitable for ancient field strength studies.

1. Introduction

Deep inside the Earth, at its core, the geodynamo controls the magnetic field that surrounds the planet and helps protect it from solar radiation. Paleointensity (PI) measurements of the magnetic field are key to constraining geodynamo models used to investigate the inner Earth. Most classic PI methods assume each specimen exhibits ideal behavior, with remanence held by noninteracting, single-domain (SD) grains, which obey Thellier's Laws of thermoremanent behavior (Thellier, 1938). Most studies on real rocks, however, have found this often not to be the case (e.g., Dunlop et al., 2005; Kosterov & Prevot, 1998; Shcherbakov & Shcherbakova, 2001). The most commonly used PI method is the Thellier-type experiment (Thellier & Thellier, 1959), which involves the simultaneous stepwise demagnetization of natural remanent magnetization (NRM) and replacement with a laboratory thermoremanence (TRM) acquired in known field. Later variants include zero-field steps either before (Coe, 1967) or after (Aitken et al., 1988) the in-field. These two

protocols can also be alternated in the IZZI protocol to detect nonideal behavior (Tauxe & Staudigel, 2004). Demagnetization and remagnetization involve numerous paired steps to increasing energy levels, typically thermal energy, but also, less commonly, alternating field (AF) steps (Shaw, 1974) or microwave radiation (e.g., Hill & Shaw, 2000). To try to mitigate non-SD grain effects, strict selection criteria have been implemented (e.g., Biggin & Bohnel, 2003; Biggin & Thomas, 2003b; Leonhardt et al., 2004a; Paterson et al., 2014). Other approaches, such as by Paterson et al. (2015), suggest excessive loss of the natural remanent magnetization (NRM) can be mitigated by increasing thermal remanent magnetization (TRM) gains by adjusting the applied field's magnitude and direction.

We used synthetic specimens containing simulated NRMs for this study to study these types of nonideal behavior as directly as possible. When given a simulated NRM, experiments can be repeated on the same specimens multiple times. Synthetic specimens have several advantages: primarily, nonideal behavior can be correlated with specific grain size intervals or domain state. Thermochemical alteration is minimized because the samples are vacuum sealed in quartz glass tubes. Further tests for alteration are systematically undertaken as repeat experiments are checked for consistency.

1.1. Nonideal Behavior

The most common magnetic mineral is magnetite, and for it to display SD behavior, its grains must be submicron in size and be well-dispersed throughout the matrix. Such rocks, however, are (very) scarce in nature, so it is therefore important to understand the behavior of non-SD grains. Our study focuses on multidomain (MD) (large grains) and interacting (poorly dispersed) grains during Thellier-style PI experiments. Repeated heating steps have been shown to affect both the remanence and the remanence capacity in an MD specimen (Biggin & Bohnel, 2003; Fabian & Shcherbakov, 2004), but oxyexsolved grains have not yet been tested accordingly. The effects of repeated heatings may be particularly important during PI experiments because they potentially cause cumulative nonideal behavior, which has been kinematically modeled by Biggin (2006).

A specimen's fundamental rock magnetic properties affect its behavior during PI experiments, leading to a nonlinear Arai plot (Nagata et al., 1963), which affects the absolute PI estimate extracted from the gradient of the resulting best-fit line. Nonideal properties often manifests itself as concave-up curvature of the ideal line, caused by alteration, (large) grain/domain size, and grain interaction; these must be identified to avoid misleading results (Coe et al., 2004; Dunlop & Ozdemir, 2001; Xu & Dunlop, 2004). Curvature can produce two-slope plots, which can lead to large overestimation or underestimation of the PI, if only the first or second slope is used, respectively (Biggin & Thomas, 2003a; Dunlop et al., 2005). The precise protocol and the number/temperatures of the points can also influence the shape (Biggin, 2006; Paterson et al., 2014; Xu & Dunlop, 2004).

The most common causes of deviation from ideal behavior by non-SD grains during a Thellier experiment according to Biggin (2006), Fabian (2001), and Shcherbakov and Shcherbakova (2001) are:

1. Asymmetry of partial TRM (pTRM) acquisition and loss (non-SD grains preferentially lose NRM over gaining TRM at low to moderate temperatures).
2. Nonreciprocal components of demagnetization and remagnetization treatments—the low and high temperature "tails" of pTRMs which change magnitude, depending on the field that imparts or removes the pTRMs, relative to the existing TRM.
3. The effect of thermal and magnetic history on the remanence of the specimen or its capacity to acquire/lose remanence—this includes pTRMs, the iterative effects of multiple treatments, and thermal history.

Each of these effects can produce concave-up Arai plots, but their relative importance is not well-known. They are qualitatively described by relatively simple phenomenological models (e.g., Biggin & Poidras, 2006; Fabian, 2001; Leonhardt et al., 2004b) but poorly understood physically (Fabian & Shcherbakov, 2004).

1.2. Grain Size Dependence

1.2.1. Interacting Grains

Subaerial basalts commonly contain grains of titanomagnetite that have undergone oxyexsolution to produce lamellae of nonmagnetic ilmenite, interspersed with near-stoichiometric magnetite. Lamellae divide up the magnetite, which results in smaller effective magnetite grain sizes. The very high aspect ratio of

these lamellae is generally interpreted by paleomagnetists to imply that they are SD in nature. Hysteresis measurements made on samples containing such grains generally plot in the Pseudo-Single-Domain (PSD) region of a Day plot (Day et al., 1977). Together, these observations are often used to argue that such specimens are likely to obey Thellier's Laws sufficiently well to reliably record the paleointensity. In addition, Almeida et al. (2016) showed that vortex state, PSD-sized magnetite particles behave comparable to SD grains in isolation.

Even if the grains are SD-like, they are close enough to magnetostatically interact. Although interaction alone has been shown not to preclude samples from being reliable geomagnetic recorders (Muxworthy et al., 2014), it has been empirically demonstrated that igneous rock samples exhibiting PSD-like behavior in high-field experiments can exhibit MD-like behavior in weak-field, i.e., PI, experiments (Biggin & Thomas, 2003a; Calvo et al., 2002; Shcherbakova et al., 2000). Recent paleointensity work on samples containing oxyexsolved titanomagnetite (e.g., Bowles et al., 2015; Shcherbakova et al., 2014) have shown that successful PI determinations can often be obtained. However, no study has yet systematically investigated pTRM behavior of specimens containing oxyexsolved grains.

1.2.2. Multidomain Grains

The remanence gained during pTRM acquisition between a given T_2 and T_1 in SD grains is the same, but in MD grains, the rock's history creates asymmetry (Shcherbakova et al., 2000). Fabian and Leonhardt (2010) found that intermediate grain sizes were more strongly biased by previous zero-field steps than larger MD and smaller (near-SD) grains were. MD grains can also have unequal blocking and unblocking temperatures, which creates asymmetry in pTRM acquisition and removal. The behavior of MD grains during demagnetization of the NRM and acquisition of a laboratory TRM has been the focus of many studies (e.g., Paterson et al., 2015; Shcherbakov & Shcherbakova, 2001; Xu & Dunlop, 2004) yet there are fewer studies focusing on the behavior of interacting grains (Cisowski, 1981; Davis & Evans, 1976; Evans et al., 2006; Muxworthy et al., 2014). The present study uses synthetic samples of natural magnetite and oxyexsolved titanomagnetite in size fractions representative of MD and interacting domain states, respectively, over a grain size range of <5 to >250 μm.

Simple models of MD TRM behavior have been used to argue that denser Thellier-style experiments (i.e., those with a larger number of steps) may produce more nonideal behavior (Biggin, 2006). If true, then paleointensity experiments would benefit from being designed to be less intense by having fewer steps with the additional benefit of a reduction in experiment time. The large number of heating steps increases the likelihood of alteration which is monitored by using repeated checks requiring further heating steps. More recent modeling work by Bowles and Jackson (2016) also suggests that cation reordering may affect a specimen's Curie temperature (T_C) and in turn cause data misinterpretation or even failure of PI experiments.

1.3. pTRM Types

The different methods used to impart a pTRM on a specimen can affect the magnitude of the remanence acquired in non-SD grains. To ensure the complete removal of a lower temperature pTRM for MD grain sizes, it is necessary to heat the specimen to its T_c in zero field, as the unblocking temperatures of specimens can frequently be close to T_c (McClelland & Sugiura, 1987).

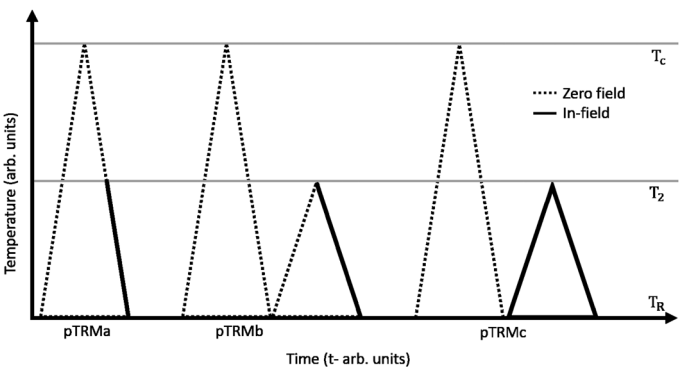

Figure 1. Three pTRM acquisition methods for a given T_2 as run in this paper. T_R can be substituted for some $T_1 > T_R$. pTRM types b and c can be run as part of a Thellier-style experiment by omitting the initial T_C demagnetization step. In pure SD grains, the three methods are equivalent (after any necessary subtractions in pTRMc).

Figure 1 shows the pTRM types as used in this study. A pTRM acquired during the cooling phase, after the complete removal of a specimen's remanence is known as pTRMa (Shcherbakova et al., 2000). A given specimen is heated to T_c and then cooling it to some T_2 in a zero field, after which time the field is switched on, until the specimen reaches T_1, where the field is turned off until reaching T_R. This process is not suitable for use in practical PI analyses, as it requires the removal of the whole remanence in the first heating step. Other methods must therefore be investigated.

The second option is a pTRMb (Shcherbakova et al., 2000), which is also referred to as $pTRM^{*,0}_{H,H_2}$ by Fabian and Leonhardt (2010). The specimen is heated to T_2 in a zero field before applying a field on cooling between T_2 and T_1 ($T_1 \in [T_R, T_2)$) after which the specimen is cooled back down to room temperature, T_R, in a zero field, if $T_1 > T_R$,

which avoids the complete destruction of the specimen's remanence. The third option, pTRMc ($pTRM^*_{H,H_2}$) is the technically simplest method (Biggin & Poidras, 2006). Samples are heated to a given T and then cooled to T_R in an applied field. The Coe (1967) variant of the Thellier method, the method used in this study, consists of double heating steps of zero-field—in-field (pTRMc) steps performed to increasing temperatures. However, lower steps must be subtracted from the higher step in order to isolate the newly acquired pTRM. Shcherbakov et al. (2001) showed that pTRMa > pTRMb. Biggin and Poidras (2006) suggested that pTRMc > pTRMb, which was later shown experimentally by Fabian and Leonhardt (2010).

Unlike ideal SD grains, which have equal blocking and unblocking temperatures ($T_b = T_{ub}$), a pTRM imparted to samples containing MD grains where $T_b \neq T_{ub}$ contains a nonreciprocal component, known as a tail. Tails cause problems in PI experiments because they are an artifact of the study that affect the inferred PI. This can be a low or high temperature tail dependent on whether $T_b > T_{ub}$ or vice versa (Dunlop & Ozdemir, 2001). These tails have been shown to be grain size dependent and to have a linear relationship (equation (1)) between pTRMb and the tail of pTRMa (Shcherbakov et al., 2001; Shcherbakov & Shcherbakova, 2001). An equivalent relationship may also exist between pTRMb and pTRMc (equation (2)). Fabian and Leonhardt (2010) found a complex relationship for a reheated pTRMc, ($pTRM^*_{H,H_2}$ in their Figure 11)

$$pTRM_a = pTRM_b + tail(pTRM_a) \quad (1)$$

$$pTRM_c = pTRM_b + tail(pTRM_c) \quad (2)$$

2. Materials and Experiments

2.1. Samples

We used 12 specimens in this study, taken from the HM4 and LM6 sets in Biggin et al. (2013), who showed the cooling rate effect on TRM intensity in samples containing oxyexsolved grains to be weak. The powders in these samples have been studied by Hartstra (1982a, 1982b, 1983). The HM4 samples consist of crushed homogeneous natural magnetite in the <5 to >150 μm size range representing large "pseudo"-SD to MD grains. For simplicity, these will be referred to as MD to specify that the grains are large but not strongly interacting. The LM6 powders contain titanomagnetite also in the <5 to >250 μm size range. Scanning Electron Microscopy images and Energy-dispersive X-ray spectroscopy (EDS) (examples in Figure 2) show that the powders appear contain titanium-rich lamellae, which subdivide the grains into interacting magnetic regions. The larger-grained oxyexsolved titanomagnetite specimens consist of an iron-rich mineral with at least two generations of lamellae. Consistent with the findings of Hartstra (1983), EDS point analyses undertaken at the University of Liverpool spectroscopy laboratory showed that the largest (presumed to be first generation) lamellae contain a more aluminum-rich titanomagnetite, probably hercynite and the finer lamellae of ilmenite. Most first generation and some second-generation lamellae do not appear to intersect, which implies that the magnetite-rich zones do not always form discrete blocks. The smallest blocks visible are <1 μm, but the lack of discretization means the effective domain state may be non-SD. The lamellae appear to be up to 300 nm thick. The degree of oxyexsolution is class C3–C4 of Haggerty (1976).

The sieved size fractions were pressed into salt pellets and vacuum sealed in evacuated quartz capsules with a length and diameter of 10 mm. All encapsulated samples were then heated to 700°C to stabilize their magnetic properties and to reduce the internal stress of the grains (Biggin et al., 2013). Checks for alteration were carried out throughout all experiments reported here by comparing the remanence intensities of TRMs and pTRMs at coincident temperature steps. The average standard error of pTRMs for all samples at coincident temperatures was 1.9%, so the alteration is deemed marginal, if present at all.

Biggin et al. (2013) ran rock magnetic experiments on these encapsulated powder samples, before they underwent any heating. Table 1 contains the pertinent rock magnetic data extracted from their experiments and TRM data from our experiments. All the data are plotted on a Day plot in Figure 3, which shows they all fall in the PSD-MD range. The HM4 data do not lie on the theoretical SD-MD mixing curves from Dunlop (2002), but the LM6 data plot nearer. Isothermal Remanent Magnetization (IRM) acquisition, hysteresis, IRM backfield, FORC diagrams, and thermomagnetic measurements were made using a Magnetic Measurements Variable Field Translation Balance (VFTB) and a Princeton Measurements Alternating Gradient Force Magnetometer (AGFM). The FORC diagrams in Figure 4 are characteristic of multidomain grains for the HM4 specimens and for interacting grains for the LM6 specimens. The higher coercvities present in the LM6 <5 μm

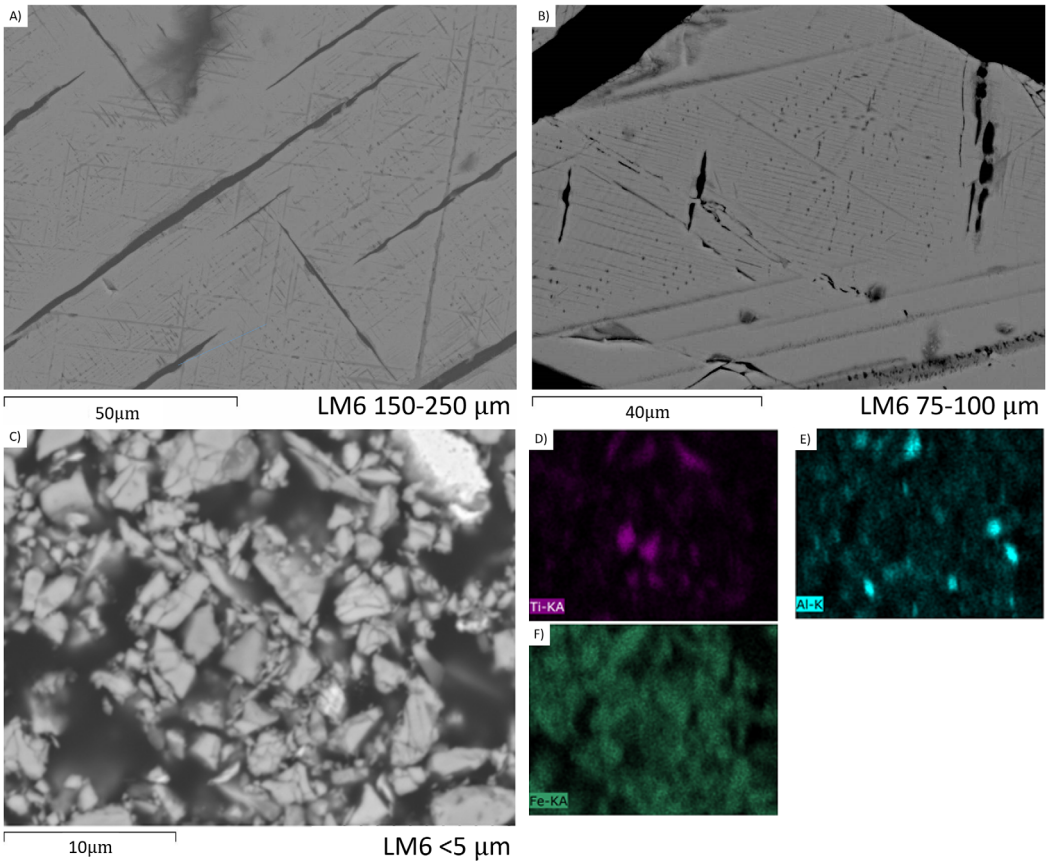

Figure 2. SEM images for LM6 powders, showing the titanomagnetite grains' lamellae. Primary, as well as some secondary and tertiary, lamellae are visible in Figures 2a and 2b. The smallest grains, in Figure 2c), have few visible lamellae. The Ti, Al, and Fe EDS maps in Figures 2d, 2e, and 2f, respectively, show that while they are all found throughout the grains, the Ti and Al appear to be concentrated in specific grains.

specimen (Figure 4c) imply that its magnetic domains have more SD characteristics than the LM6 150–250 μm specimen's domains. Combined with the LM6 SEM images in Figure 2 and the specimens' positions on the Day plot in Figure 3, we infer that the oxyexsolved grains are interacting with domain sizes in the SD to PSD-size range.

Table 1
Rock Magnetic Properties of the Specimens Used, Adapted From Biggin et al. (2013)

Name (grain size in μm)	Mineralogy	TRM at 45 μT $\left(\frac{\mu Am^2}{kg}\right)$	M_S $\left(\frac{Am^2}{kg}\right)$	M_{rs} $\left(\frac{Am^2}{kg}\right)$	H_c (mT)	$\frac{H_{cr}}{H_c}$	$\frac{M_{rs}}{M_s}$	T_C
LM6 < 5	Oxyexsolved TM	476.39	0.22	0.041	23.19	2.13	0.183	569
LM6 25–30	Oxyexsolved TM	303.18	0.44	0.034	9.91	3.44	0.076	567
LM6 75–100	Oxyexsolved TM	67.4	0.94	0.057	8.44	4.01	0.061	569
LM6 150–250 (2 specimens)	Oxyexsolved TM	284.76, 434.41	0.23	0.017	8.1	3.17	0.072	~580
HM4 5–10	Magnetite	333.84	0.44	0.029	7.6	4.05	0.066	577
HM4 15–20	Magnetite	101.58	0.26	0.009	4.32	6.01	0.034	577
HM4 25–30	Magnetite	122.63	0.18	0.005	3.9	6.66	0.03	579
HM4 40–55	Magnetite	177.16[a]	0.28	0.005	2.27	12.0	0.017	581
HM4 55–75	Magnetite	135.83	0.66	0.013	2.67	8.54	0.02	580
HM4 75–100	Magnetite	302.8[a]	0.57	0.011	2.81	9.72	0.02	578

[a]Average of two specimens.

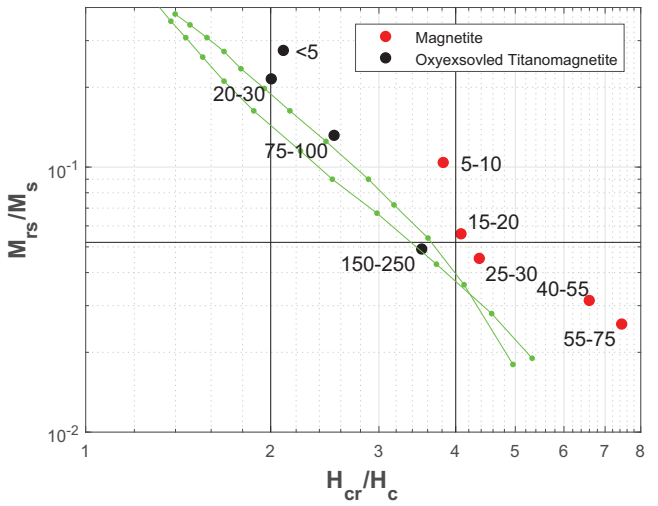

Figure 3. Day plot showing the specimens detailed in Table 1. Pure magnetite specimens are in the large PSD/MD range and the oxyexsolved titanomagnetite specimens are in the medium-large PSD range. The grain sizes are given in μm. The green curves are the SD-MD mixing curves from Dunlop (2002). The oxyexsolved specimens plot close to the curves and therefore appear to be explainable to first order as mixtures of SD and MD grain sizes, which are consistent with the SEM images. The magnetite specimens plot further away, potentially due to some superparamagnetic grains becoming attached to the larger grains during sieving.

2.2. Experiments

Experiments reported in the present study were designed to identify the grain size dependency relating to pTRM acquisition and loss, thermal history, and the iterative effects of multiple in-field heating steps at the same temperature. A series of Thellier-Coe PI experiments were performed, from known starting conditions, to calculate the magnitude of nonideal behavior, which could be associated to nonideal behavior relating to grain size and domain state. The Thellier-Coe experiments (Table 2) aimed to investigate the behavior of the synthetic samples and their dependence on the number of steps used, the choice of the initial start temperature, and grain size and type.

All experiments were carried out at the Geomagnetism Laboratory at the University of Liverpool (UK). Care was taken to precisely replicate the treatments with the same temperatures, applied field, and hold and measurement times. Two ovens were used in this study: the Magnetic Measurements Thermal Demagnetizer Super Cooled oven (MMTDSC) and a 16 specimen capacity Magnetic Measurements Thermal Demagnetizer. The results of identical experiments performed in both ovens were checked and found to be equivalent. The use of the Magnetic Measurements Supercooled oven meant experiment time was reduced and temperature was controlled to 0.3°C precision, making it possible to apply 2°C or 3°C steps. All magnetic remanence measurements were made on a Tristan Technologies cryogenic magnetometer, and an applied field of 80 μT was used to give a full TRM and during in-field steps.

We ran eight different types of experiments in this study (cf. Table 3).

a. Two types of pTRM (pTRMb and pTRMc, as shown in Figure 1) were imparted after, in each case, the samples were first fully demagnetized by cooling them from 600°C to room temperature in zero field. Fabian and Leonhardt (2010) completed a similar pTRM study as part of a multispecimen PI protocol (MSP) framework. To impart a pTRMb (Shcherbakova et al., 2000), specimens were then heated to 500°C, held for 20 min in a zero field, before applying a field of 80 μT and cooling back to room temperature. To impart a pTRMc (Biggin & Poidras, 2006), specimens were treated identically, except that the heating to 500°C and subsequent cooling were all performed in an applied field of 80 μT. We also performed additional partial demagnetizations to test if the tail of pTRMc and pTRMb (equation (2)) has an equivalent relationship to the Shcherbakov and Shcherbakova (2001) relationship between the tail of pTRMa and pTRMb (equation (1)).
b. This experiment aims to quantify the excess loss/gain of NRM that could occur during identical repeated heating treatments (Biggin & Bohnel, 2003) and also to test the first-order symmetry of pTRM behavior, as outlined in Biggin and Poidras (2006), which is important not only for Thellier-style PI experiments, but also for the MSP. Specimens were given a full TRM, then thermally demagnetized at 500°C and measured at room temperature. This partial thermal demagnetization process was repeated an additional two times. The symmetrical experiment was then performed: samples were fully demagnetized, given a pTRMc at 500°C, cooled to room temperature, and measured. The remagnetization step was repeated another two times to see if the result differs as a result of pTRMc changes.
c. The same as experiment (b) but with a peak demagnetization/remagnetization temperature of 540°C.
d. (d–g) Simulated Thellier-Coe experiments from a full TRM at 80 μT using different numbers of steps (8–14) and initial start temperatures (500–565°C) until the Curie Temperature in equally spaced steps (2–6°C), see Table 2 for breakdown. The actual temperature at each step varies by specimen based on $T_{initial}$ and the specimen's T_c.
e. (h or Full) A simulated Thellier-Coe experiment incorporating the whole temperature range including pTRM checks (Prévot et al., 1981) and tail checks (Riisager et al., 2001), which will be referred to as the full Thellier/Coe experiment from here on. It is used as a benchmark for comparison with other simulated Thellier/Coe experiments.

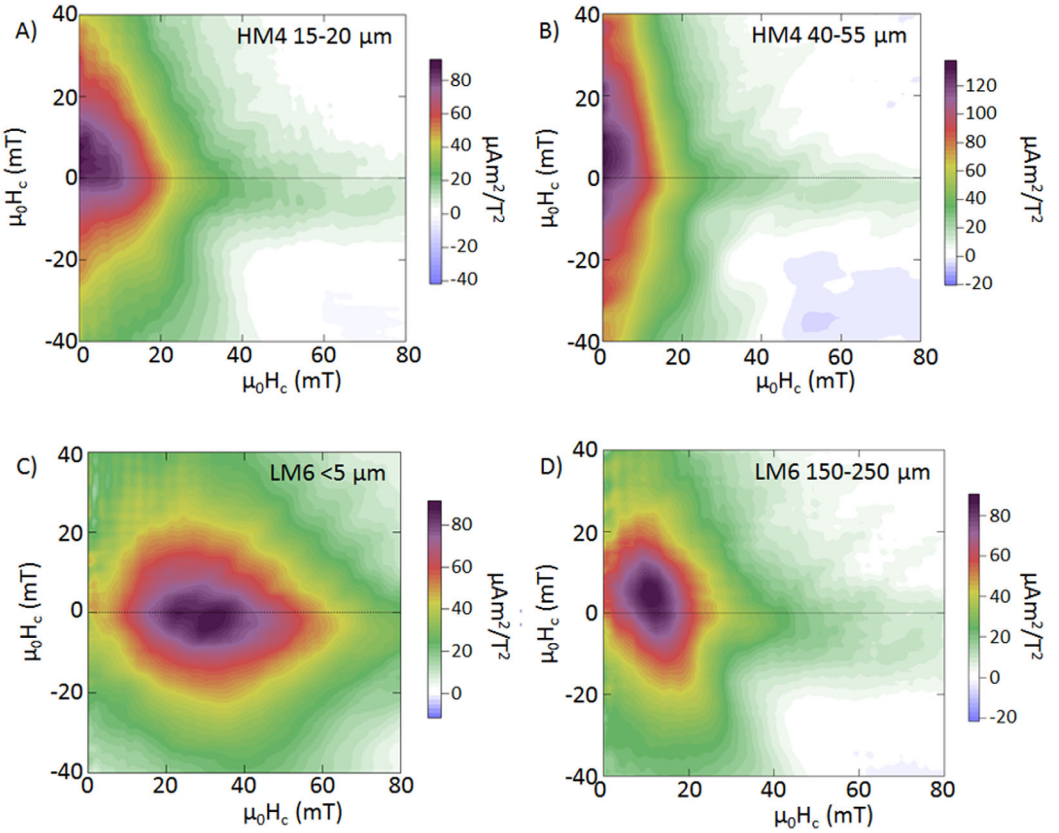

Figure 4. FORC diagrams representative of the (a and b) MD and (c and d) oxyexsolved specimens. The data used are the same from (Biggin et al., 2013) but re-evaluated using FORCinel (VARIFORC method not used) with a smoothing factor of 9, increasing at a rate, λ=0.1, as H_C increases (more smoothing at points farther away from the main area of interest) (Harrison & Feinberg, 2008).

3. Results

3.1. Experiment (a): Acquisition of pTRMb and pTRMc

The magnitude of remanence gained during pTRMc was larger than that using the pTRMb method for all specimens and thus all grain sizes (Table 3). On average, pTRMc was 4.9 ± 0.5% larger in oxyexsolved specimens and 6.2 ± 0.3% larger in MD specimens, with an average increase of 5.5 ± 0.5% for the two series of samples, across the entire grain size range. The error is calculated as standard error of the mean (SE). Oxyexsolved specimens display a grain-size dependence: larger grains have larger differences. MD grains do not display a grain-size dependence, which can be seen in the clustering in Figure 5, in which the remanence of pTRMc against pTRMb plus the tail of pTRMc is plotted. For oxyexsolved specimens, the sum of pTRMb and

Table 2
Summary of Experiments Discussed in This Paper

Experiment	Description	(N) steps or iterations	Start temperature (°C)
a	pTRMb versus pTRMc acquisition	n/a	500
b	Iterative demagnetization/remagnetization	3	500
c	Iterative demagnetization/remagnetization	3	540
d	Thellier-Coe experiment	14	500
e	Thellier-Coe experiment	14	557
f	Thellier-Coe experiment	10	565
g	Thellier-Coe experiment	8	500
h, Full	Thellier-Coe experiment incl. tail and pTRM checks	38–46	100

Table 3
Summary of the Results From Experiment (a)

Sample size (μm)	pTRMc (%)	A_c (500, T_r) (%)	pTRMb (%)	A_b (500, T_r) (%)	Δ (pTRMc, pTRMb) (%)	pTRMb + (tail)pTRMc (%)	pTRMc − (pTRMb + (tail)pTRMc) (%)
Oxyexsolved							
LM6 < 5	18.35	14.23	15.41	9.61	2.94	18.02	0.33
LM6 25–30	19.54	16.39	14.64	11.78	4.9	17.84	1.7
LM6 75–100	21.23	22.58	16.28	18.26	4.95	21.07	0.15
LM6 150–250	25.71	17.72	19.94	14.05	5.77	24.49	1.22
LM6 150–250	28.47	19.13	22.54	16.05	5.93	27.99	0.49
MD							
HM4 5–10	17.54	16.76	12.02	13.75	5.53	14.96	2.59
HM4 15–20	17.05	14.83	11.49	16.83	5.56	14.02	3.03
HM4 25–30	17.28	19.57	11.31	15.12	5.97	14.7	2.58
HM4 40–55	19.8	15.95	12.7	21.19	7.11	15.85	3.95
HM4 55–75	17.32	23.99	10.68	20.2	6.64	14.84	2.48

Note. Experiment (a) compares the pTRMb and pTRMc methods of pTRM acquisition at 500°C. All reported values are normalized to the full TRM value of each sample. Ab(500,T_R) Ac(500,T_R) are the ratios of the tail to the pTRM from Shcherbakov et al. (2001). Δ(pTRMc, pTRMb) is the difference between pTRMc and pTRMb.

the tail of pTRMc is 0.8 ± 0.3% smaller than the equivalent 1:1 relationship, compared to that seen in equation (3). For MD specimens, the sum of the two components is on average 2.9 ± 0.3% less than when pTRMc was used. To provide additional domain state data, we used the A_c and A_b variables from Shcherbakov et al. (2001), as given by

$$A_x(T_2, T_1) = \frac{tail(pTRM_x(T_2, T_1))}{pTRM_x(T_2, T_1)} \quad (3)$$

notation adapted from Shcherbakov et al. (2001).

This ratio has been shown to be an indicator of domain state from SD to MD, when the pTRMa method of acquisition is used. We determined ratios from tails and pTRM's acquired at 500°C using the pTRMc method of acquisition (analogous to the experiments described in Shcherbakov et al. (2001)). Unlike their data, which plot in discrete boxes, ours are more continuous across the spectrum, as shown in Figure 6. The grain size dependency is not apparent using these ratios, so these ratios are of less use than those reported in Shcherbakov et al. (2001).

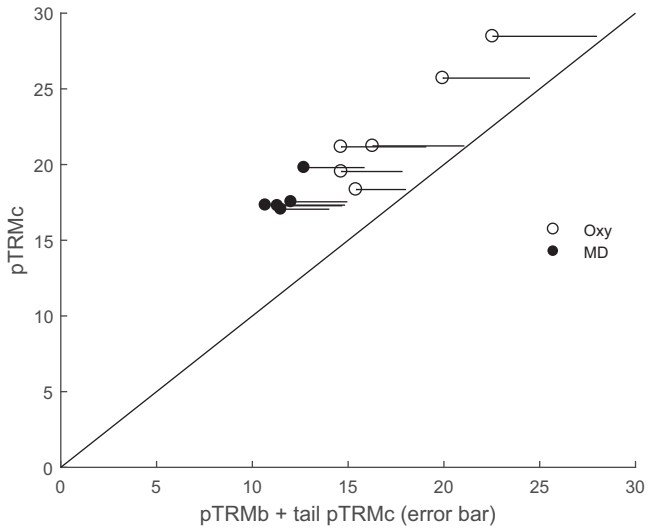

Figure 5. pTRMc plotted against pTRMb (circles) + tails of pTRMc (horizontal bars) at 500°C. Values on axes represent percent of full TRM.

3.2. Experiments (b) and (c): Iterative pTRM Acquisition/Loss at 500°C and 540°C, Respectively

Experiments (b) at 500°C and (c) at 540°C aim to isolate the effects of repeated heating and cooling on specimens, independent of a change in temperature. For all specimens, more NRM is lost during the demagnetization step than TRM is acquired during the equivalent remagnetization step. Figure 7 shows a selection of typical results from the experiment.

Figure 7 further demonstrates that each iteration of the experiment causes an increased deviation from ideal behavior. At 500°C, MD samples lose an additional 7.3 ± 0.3% of NRM and gain an additional 2.1 ± 0.2% TRM compared to the oxyexsolved samples which lose 5.5 ± 0.3% NRM to 2.7 ± 0.2% TRM gain over the iterations. The iterative effects compound the loss of symmetry: after all three steps, the total difference of NRM lost and TRM gained at 500°C is 14.7 ± 0.8% in MD samples and 8.4 ± 0.4% in oxyexsolved samples. At 540°C, the total difference is 15.3 ± 1.3% in MD samples and 7.1 ± 0.8% in oxyexsolved samples after the iterations. Figure 8 compares the total

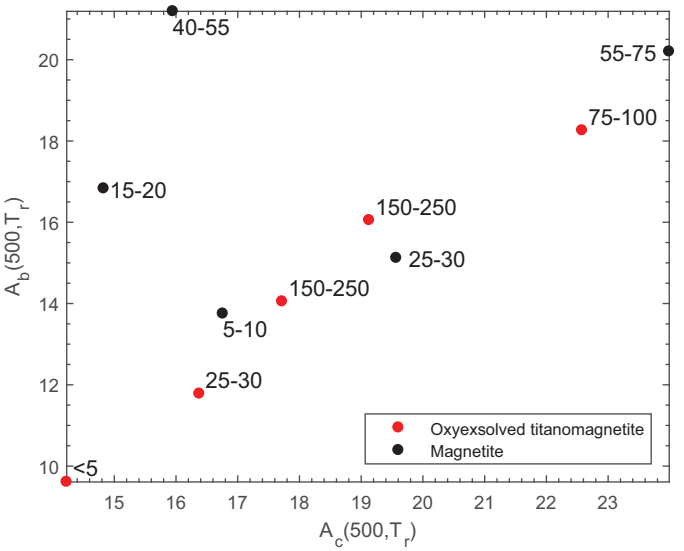

Figure 6. $A_b(500,T_r)$ versus $A_c(500,T_r)$ for our specimens. Unlike the data in Shcherbakov et al. (2001), our specimens do not plot within discrete boxes. Our oxyexsolved titanomagnetite data appear to form a line and the MD magnetite appear to be scattered around the plot.

differences, the initial disparity at step 1, and the iteration's effects as a function of grain size. Separating the effects of the iterations from the initial difference in NRM loss to TRM gain shows that MD grains have larger iterative effects than the oxyexsolved grains, but also that grain size is less important than whether they are MD or interacting.

The proportional difference between the NRM loss and TRM gain at the first heating step, can be referred to as this nonreciprocal component of remanence, which is measured as:

$$\Delta = \frac{NRM_{lost,1} - TRM_{gain,2}}{NRM_0} \quad (4)$$

The nonreciprocal component is distinct from a tail because the NRM loss and TRM gain are measured from different experiments, which had different thermal histories. The nonreciprocal component results from failure of Thellier's Law of Reciprocity (i.e., $T_{ub} \neq T_b$). The nonreciprocal component results are summarized in Table 4. The results are averaged as no clear grain-size dependence was observed in the data.

3.3. Experiments (d–g): Simulated Thellier-Coe Experiments

Experiments (d–g) are simulated Thellier-Coe experiments that use different starting temperatures and numbers of steps. The results of experiments with fewer steps have been compared to the full simulated Thellier-Coe experiment, which covered the whole temperature range, including checks and involved up to 46 heating steps.

NRM loss is lost evenly across the experiment, whereas TRM acquisition is concentrated at higher temperatures, as shown in Figure 9. TRM acquired typically remains below 20% until around 20°C before Curie temperature when it increases rapidly. These experiments showed strongly nonideal behavior in the oxyexsolved specimens. NRM is preferentially lost at lower temperatures and TRM is preferentially gained at higher temperatures, so when the curves from Figure 9 are plotted against each other in an Arai plot, the plot becomes concave-up. Figure 10 shows the resulting nonlinear, concave-up behavior observed in both oxyexsolved and MD grains. There does not appear to be a simple correlation between grain size and linearity of the Arai plots for the oxyexsolved specimens. For example, LM6 75–100 has the least linear Arai plot for the 500–560°C test, whereas LM6 150–250 has the least linear Arai plot for the full experiment. The MD specimens appear to have Arai plots with significantly higher curvature.

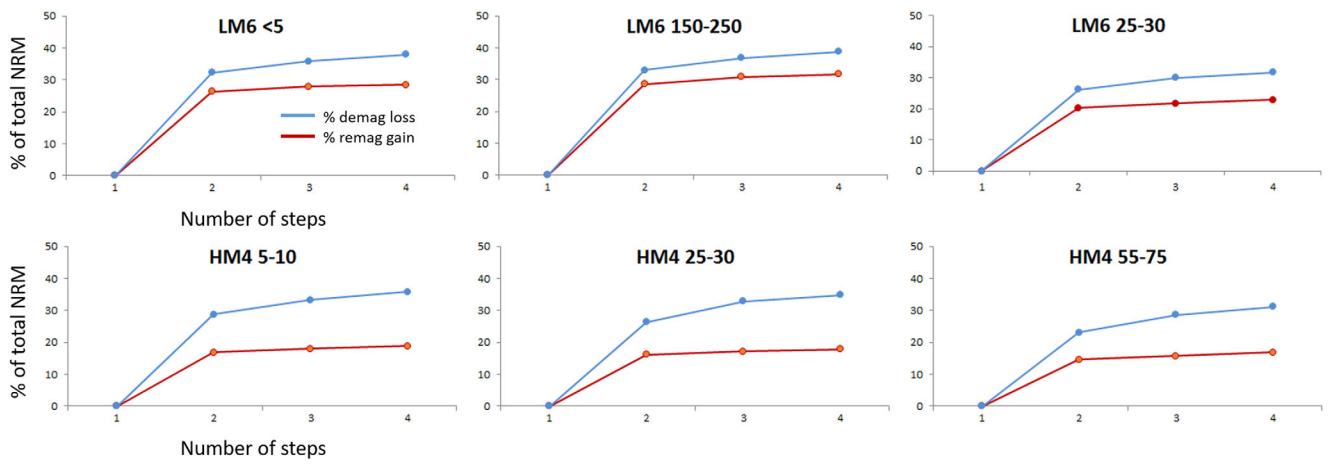

Figure 7. The iterative effects of repeated heating for demagnetization and remagnetization at 500°C. Top rows are oxyexsolved samples and bottom rows are MD.

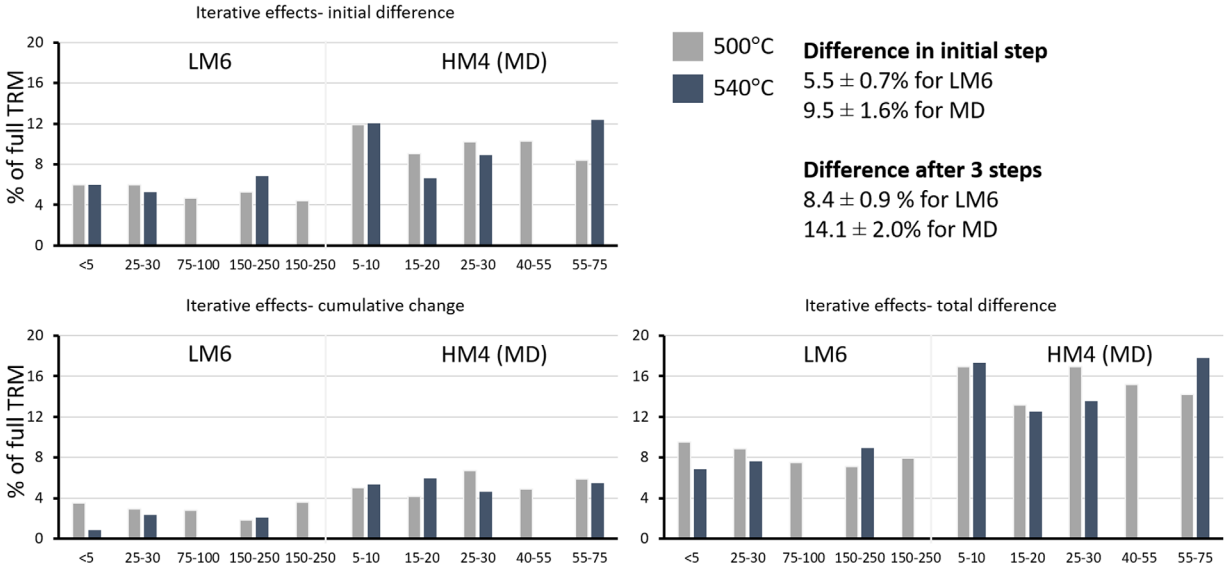

Figure 8. The normalized difference between the TRM and NRM curves in Figure 7. (a) The total difference after all three steps, averages = 8.4 ± 0.9% for oxyexsolved grains and 14.1 ± 2.0% for MD and (b) the initial disparity in NRM lost to TRM gained averages = 5.5 ± 0.7% for oxyexsolved grains and 9.5 ± 1.6% for MD.

At high temperatures, the deviation of the points from the ideal 1:1 line began to decrease (Figure 10). This increased NRM loss also leads to an apparent lowering of the Curie temperature in the full experiment. As the initial temperature increased all the points move toward the ideal line, exemplified by experiments (e) and (f). These experiments used initial temperatures of 557°C and 565°C and 3°C and 2°C heating steps, respectively. Experiment (f) was generally unsuccessful. Figure 10 further shows that more NRM remains at higher temperatures when fewer low-temperature steps are run, with some representative 500°C and 560°C steps marked. If the lower temperature portion of the plot is used, the PI estimate is between 70% and 185% overestimated. Figure 11 confirms that this pattern holds for all experiments run with higher starting temperatures. For samples only given high temperature treatments and no low-temperature treatments, the mean difference in NRM lost at a given temperature is 6.5 ± 3% lower in the oxyexsolved specimens and 14 ± 3% lower in the MD specimens. The TRM gained during the full experiment was <5% higher than those whose initial temperature step was 500°C, which suggests that only minor alteration is occurring. The small difference in TRM gained means that more accurate data are extracted when only high temperatures are used for the experiments.

4. Discussion

4.1. Key New Findings

The oxyexsolved specimens show behavior usually associated with MD grains during the pTRM acquisition and the iterative loss experiments. Oxyexsolved specimens show a grain-size dependence for pTRM acquisition, which implies that larger grains interact more strongly with each other when the lamellae size remains constant. MD grains behaved as expected. The effective grain size of the oxyexsolved samples is in the SD to PSD range. Nonideal behavior is likely a combination of interaction between the closely spaced magnetic domains and potentially the magnetic grains themselves, as they are often nondiscrete. In these experiments, the behavior manifests as concave-up slopes in the Arai plots of simulated Thellier-Coe experiments.

We have found that pTRMc > pTRMb in both MD and oxyexsolved specimens (Figure 5) and that equation (2) holds within 3% for MD specimens and within 1% for oxyexsolved specimens. Both MD and oxyexsolved grains lose more NRM than gain TRM at temperatures up to 540°C; this is a cumulative effect.

Table 4
Summary of Average Results From Repeated Heating Experiments

	Initial Δ (%)	Iterative gain (%)	Iterative loss (%)	Total Δ[a] (%)
Oxy 500	5.5	2.7	5.6	8.4
Oxy 540	5.9	4.8	6.0	7.1
MD 500	9.5	2.1	7.2	14.7
MD 540	9.9	2.5	7.8	15.3

[a]The total difference after multiple heating steps is consistently larger than the initial difference, which means the iterative effects are cumulative.

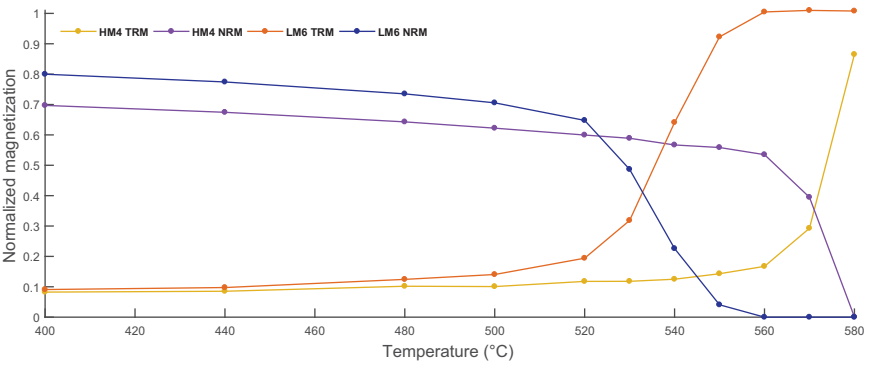

Figure 9. Demagnetization versus remagnetization curves representing both MD and oxyexsolved grains. The remagnetization curve lags the demagnetization curve until the last couple steps (corresponding to temperatures within 20°C of T_C).

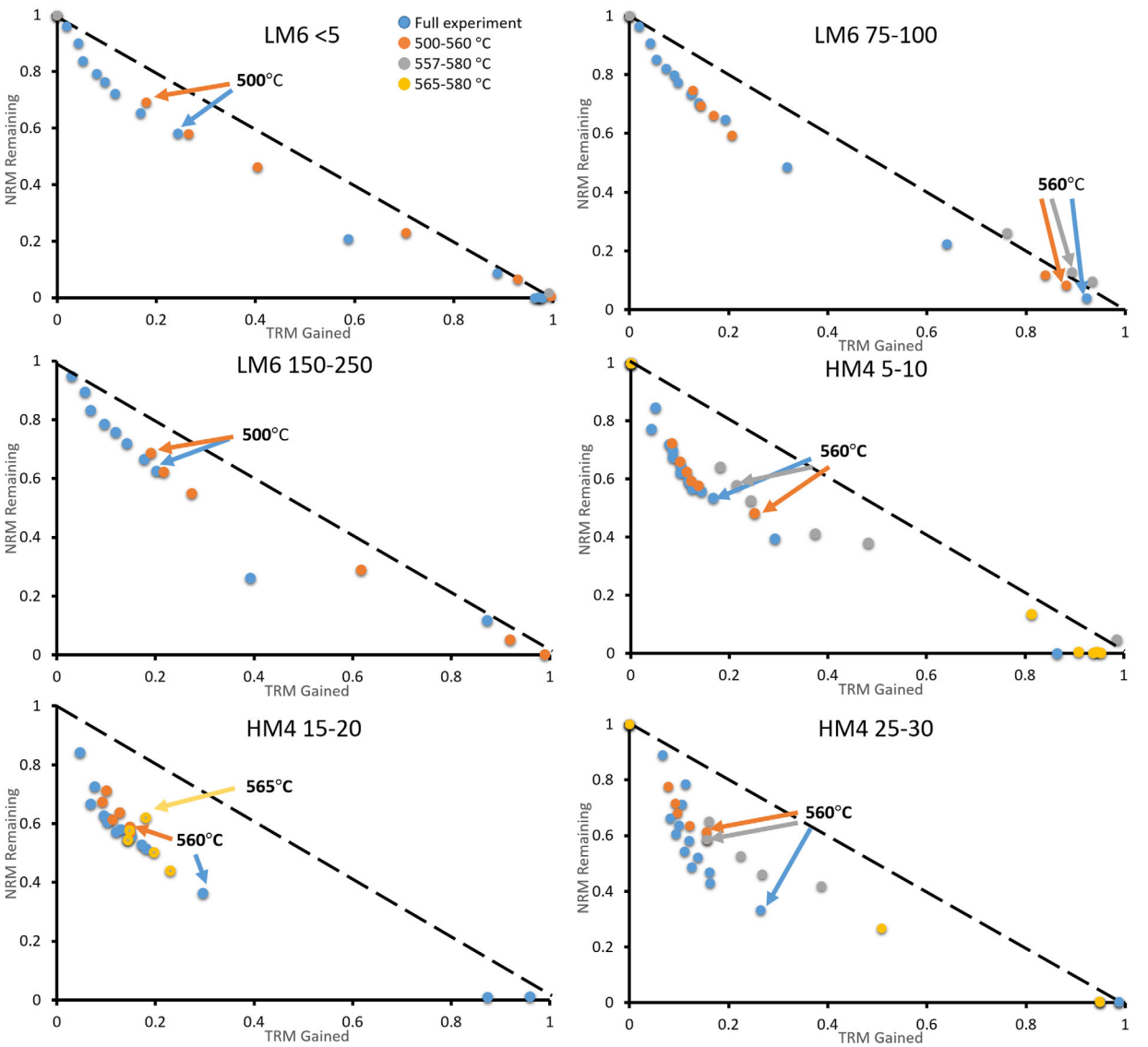

Figure 10. Examples of the experiments (d)–(g). In all experiments, the applied field was the same as the original field so the ideal (dashed) line represents the gradient required to obtain a correct paleointensity value. Blue circles are the full simulated Thellier experiment.

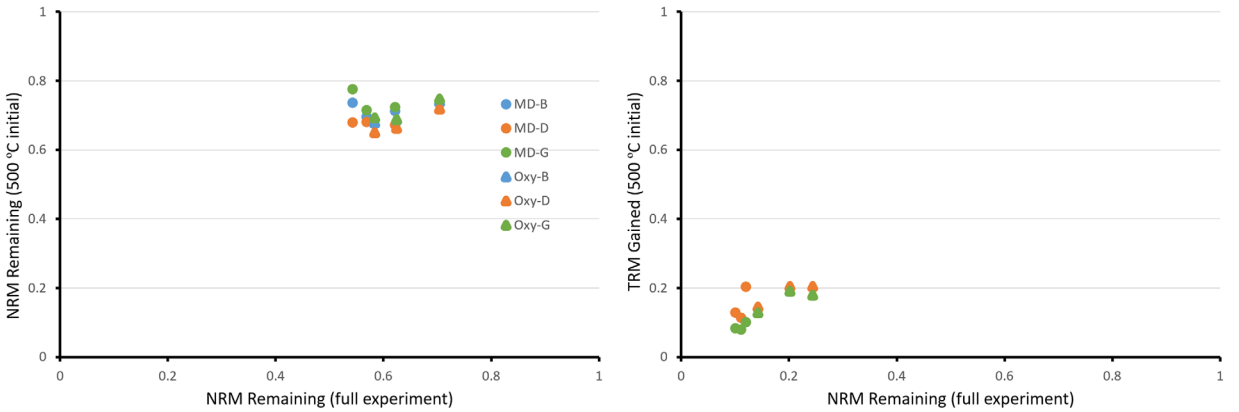

Figure 11. (left) Comparison of NRM remaining at 500°C in full Thellier-Coe experiments (NRM 1) and all experiments where 500°C was the first step (NRM 2). (right) TRM gained by 500°C in the same experiments. Experiment (b) is excluded from this plot as it underwent a different thermal history and was not comparable for TRM gain.

4.2. pTRM Types

Previous studies comparing pTRMa and pTRMb acquisition methods have shown that pTRMa > pTRMb (Shcherbakova et al., 2000) and that there is a linear relationship between pTRMb and the tail of pTRMa (equations (1) and (2)) (Shcherbakov & Shcherbakova, 2001). Fabian and Leonhardt (2010) determined that the differences in pTRMb and pTRMc are sufficiently large as to cause the MSP method to fail if zero-field steps are used. Our data further show that pTRMc is consistently greater than pTRMb, independently of the specimen's grain types or domain state. We found the peak difference was for HM4 55–75, the second largest MD grain size tested. These grains are much larger than Fabian and Leonhardt (2010)'s specimen with the highest deviation, W4 (5.7 μm).

Unfortunately, it was not practically possible to reliably measure a pTRMa for comparison, and the specimens have since broken. Since there is no apparent grain size correlation we can take averages of the differences without losing data; pTRMc is greater than pTRMb by 4.9 ± 0.5% in the oxyexsolved grains and 6.2 ± 0.3% in the MD with an overall average of 5.5 ± 0.5%, independent of domain state or grain size (for oxyexsolved and MD grains). In terms of remanence acquisition, the oxyexsolved and MD specimens behave similarly. Equation (2) appears to be accurate within 0.8 ± 0.3% for oxyexsolved grains and within 2.9 ± 0.3% for MD grains. A_c(T2,T1) and A_b(T2,T1) values extracted from tails and pTRMs acquired at 500°C, using the pTRMc method of acquisition, have comparable magnitudes to those acquired at 300°C using pTRMa in Shcherbakov et al. (2001). Though the temperatures are different, this suggests another instance in which pTRMc is comparable to pTRMa.

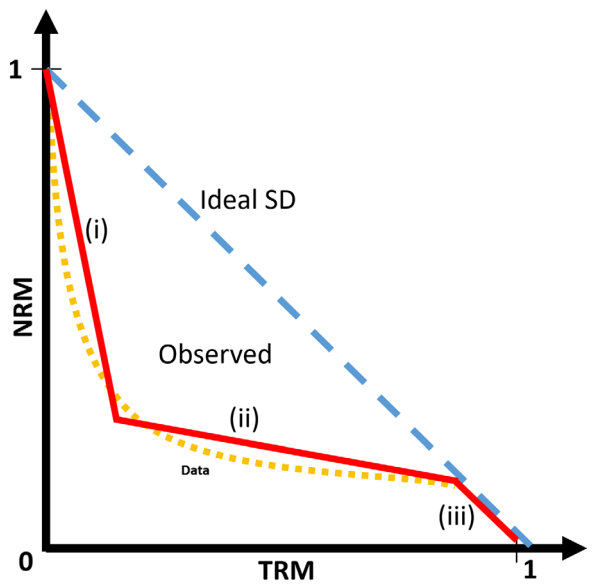

Figure 12. Simplified graph depicting the behavior observed and described in Table 5. At low temperatures, (i) NRM is preferentially lost, then (ii) TRM is preferentially gained, before (iii) the two finally equilibrate near T_C. The red line is our discretization of our collected data in yellow.

4.3. Iterative Effects and Symmetry

The size of the nonreciprocal element given by equation (4) was 72% larger for the MD grains than for the oxyexsolved specimens at the first step. After the repeated heatings, both MD and oxyexsolved grains have larger deviations, but the difference was a comparable 68%, which implies that the deviations increase proportionally as the heatings are repeated. Imparting a pTRM on a specimen with a full TRM appears to be more effective than imparting a pTRM on a partially demagnetized specimen.

The observed Arai plots show similar concave-up curves for both MD and oxyexsolved grains. The resulting asymmetry of NRM loss/TRM gain is contrary to previous findings on natural specimens, which show symmetric behavior (Biggin & Poidras, 2006; McClelland &

Sugiura, 1987). Typically excesses in NRM loss to TRM gain level off exponentially with increasing temperature steps (Figure 9). The magnetization becomes more stable, most likely due to stabilization of domain state from repeated heat treatments (Fabian & Shcherbakov, 2004), as larger (PSD-sized) magnetite can exist in a vortex state, which is stable up to its T_C (Almeida et al., 2016).

McClelland and Sugiura (1987) measured remanence at high temperature and again at room temperature in non-SD grains and showed that excessive loss of NRM occurs during the cooling stage of a zero-field step. In our experiments, there is a strong domain state dependency at the two temperatures tested (500°C and 540°C), which is seen in Figure 7 and Table 4. However, when the data are corrected for the iterative effects, the observed curvature does not change significantly, which implies the additional NRM loss from iteration is minimal in these specimens.

Our experiments show more NRM remaining at 500°C when 500°C is the initial step, compared to the full experiment with multiple steps prior to 500°C. This confirms that thermal history in both oxyexsolved and MD grains affects the remanence. Due to metastability being a function of temperature, the domain configuration changes if a temperature is reached incrementally, after repeated heating/cooling cycles, or in a single heating step. Our results here thus agree with Dunlop (2009) and McClelland and Sugiura (1987), which showed that NRM is lost less quickly during continuous heating. A high initial starting temperature can potentially be considered as an intermediate between a continuous experiment and a stepwise experiment, with NRM losses minimized until the most linear portion of the Arai plot. Our data further show that smaller-sized MD grains have both a larger initial difference and total difference after repeated heating/cooling cycle, but potentially as a result of our heatings being all in-field, the intermediate grain size bias observed in Fabian and Leonhardt (2010) did not appear in these data.

The converse is also true for the TRM gained. More low-temperature steps causes more TRM gain than from a single step, but the effect on TRM gain is more moderate than on the NRM loss. Yu and Tauxe (2006) and McClelland et al. (1996) noted that multicycle heatings for in-field steps caused a progressive increase in pTRM acquisition in coarse grained magnetite. Our data demonstrate their results apply to oxyexsolved grains as well.

Our data can also help expand the results of Fabian and Leonhardt (2010) for the multispecimen PI protocol (MSP). Both oxyexsolved and MD grains are prone to excessive loss of NRM and low TRM gain at temperatures used for the MSP (i.e., those unlikely to cause alterations). Their method of normalization, MSP domain-state corrected (MSP-DSC), using their pTRM*(*T*) (our pTRMc) will likely work for oxyexsolved grains of comparable sizes, but since we did not run any MSP experiments, our data are insufficient to confirm this outright.

4.4. Implications for Thellier-Style Experiments

For all the experiments, we observed concave-up Arai plots, which are characteristic of nonideal behavior and in our case are not due to thermochemical alteration. At lower temperatures, NRM is preferentially lost and TRM generally remains below 20%, until Ts = Tc – 20°C. At this temperature, generally 70% of the NRM has been lost. Xu and Dunlop (2004) used synthetic specimens containing homogeneous MD magnetite. They observed a consistent pattern in their Arai plot data (detailed in Table 5 and Figure 11) that is comparable to our observations for MD specimens. Oxyexsolved specimens showed a similar pattern but slightly different temperature bounds. Increasing the initial temperature of the PI experiment to 500°C showed a 67 ± 8% decrease (from 0.60 to 0.19) in curvature for oxyexsolved grains and a 25 ± 7% decrease (from 0.92 to 0.68) in curvature for MD grains, using the $|\vec{K}'|$ definition from Paterson et al. (2014), with no apparent grain size dependence. Increasing the starting temperature further, to 557°C, decreases curvature by 89% for the

Table 5
Nonideality in Arai Plots Compared to Temperature Ranges (in °C) for Pure Magnetite

Effect observed	Xu and Dunlop (2004)	MD specimens	Oxy specimens
NRM loss > TRM gain (i)	<540	<540±6	<530±3
NRM loss < TRM gain (ii)	540−565	540−560	530−550
NRM loss = TRM gain (iii)	565−580	560±6−580	550±5−580

single oxyexsolved specimen (from 0.52 to 0.057) and 64 ± 3% (from 0.98 to 0.36) for the two MD specimens that had sufficient NRM remaining to be studied using this method.

Natural samples containing grains comparable to the oxyexsolved sample set used here are commonly used in PI experiments, which means that nonideal behavior could cause overestimations in absolute PI values. The lower temperature section of an Arai plot is commonly used to avoid nonideal behavior that might be caused by alteration at higher temperatures (i.e., Kosterov & Prevot, 1998), but more recent work, e.g., Biggin (2010) and Smirnov et al. (2017) has shown that using the low-temperature portion of a concave-up Arai plot from a Thellier-style experiment can lead to large PI overestimations. These experiments indicate that the majority of the nonideal behavior occurs in the low-temperature portion of the Arai plot. The result is an overestimation in PI values using the low-temperature range and an underestimation in the high-temperature range.

Our simulated Thellier-Coe experiments have demonstrated that modifying the initial temperature step in a Thellier experiment changes apparent nonideal behavior, but that nonideal behavior exists throughout nearly the entire temperature range. These Thellier experiments indicate the majority of the observed nonideal behavior occurs in the low-temperature (first few steps) portion of the Arai plot. The higher temperature portion of the plot shows less curvature when there has been less excessive NRM loss at the lower temperature steps. The temperature of the first step is key in avoiding erroneous PI values, even when the high temperature portion of the Arai is used.

Excessive remanence loss during the cooling phase of the zero-field step is avoided when a single heating protocol is used such as the less commonly used Wilson (continuous heating to T_c) (Muxworthy, 2010; Wilson, 1961) or Shaw (AF and ARM calibrated with a single TRM) (Shaw, 1974) methods. The single heating also avoids the use of pTRMs and is therefore expected to be independent of grain size. Continuous and stepwise demagnetization have been shown not to be equivalent in MD grains (Dunlop, 2009). During a stepwise experiment, NRM is lost incrementally over the whole temperature range, but during a continuous experiment, the NRM is relatively stable up to the minimum blocking temperature. Excess remanence is lost during the cooling down to Tr in the zero-field step of a stepwise experiment, which does not occur during continuous demagnetization, which provides a potential explanation for why more NRM remains after 500°C if there are no prior steps. By using a high initial temperature, a specimen can be considered to have been continuously demagnetized to the initial temperature, e.g., 550°C, and then stepwise demagnetized to its Curie temperature. Ideally, the initial temperature step of any Thellier experiment needs to be higher than the point at which NRM is preferentially lost over TRM gained. One such method is to identify the inflection points is stepwise demagnetizing a sister specimen and remagnetizing with pTRMs.

Previous works (e.g., Kosterov & Prevot, 1998; McClelland et al., 1996; Shcherbakov & Shcherbakova, 2001; Xu & Dunlop, 2004) have suggested that as the Curie Temperature is approached, the total NRM loss to total TRM gain becomes more symmetrical, $T_{ub} = T_b$, so the points on an Arai plot should plot closer to the ideal straight line. We also observed this in our experiments. Increasing the temperature of the initial double step (up to $557°C < T_c - 20°C$) in the experiment caused every point to shift toward the ideal line (Figure 10), which implies that nonreciprocity early in the experiment permeates through the whole experiment.

Since our oxyexsolved data show remarkably similar behavior to our MD data, the five recommendations made by Biggin (2006) to minimize nonideal behavior in double-heating experiments are just as relevant for assemblages of oxyexsolved grains as for their MD equivalents, with a single possible exception. As $T_i \rightarrow T_c - 20$, the curvature decreases, which means that using $T_I \approx T_c - 20°C$ and small temperature intervals (~3°C steps) potentially reduce curvature the most, but can increase clustering. All Thellier-type experiments should be accompanied by appropriate checks for nonideal behavior that include pTRM checks, the $|\vec{K}|$ or $|\vec{K'}|$ parameter (Paterson, 2011; Paterson et al., 2015), pTRM tail checks (Riisager & Riisager, 2001), and/or the IZZI protocol (Tauxe & Staudigel, 2004). Although we did not utilize such checks in this study, nothing in our results questions their efficacy. We further note that the stronger TRM carried by small fractions of noninteracting single-domain grains in rock samples may magnetically smother the effects from nonideal carriers such as those carried here.

5. Conclusions

Both the MD and interacting oxyexsolved specimens preferentially lose NRM during cooling of zero-field steps in PI experiments, but repeated heatings only have a weak effect over an entire experiment. Since

interacting grains are common, natural specimens containing them can thus potentially give erroneously high PI estimates. Higher initial temperatures can be used to minimize the excess NRM loss from lower temperature steps. During simulated Thellier experiments, when $T_i = T_c - 20°C$, Thellier's Laws of reciprocity, additivity and independence are satisfied. This temperature fraction behaves SD-like, with $T_b = T_{ub}$, which suggests using only this range is suitable for PI experiments, but alterations are much more likely to occur before the first temperature is reached.

Samples containing purely oxyexsolved titanomagnetite are subject to some of the same sources of non-ideal behavior as are those of homogeneous magnetite. Checks for MD-like behavior should be applied to specimens with hysteresis properties like those in this study. A better understanding of the rock magnetic properties of any given sample will aid in devising a suitable experiment. Unlike for SD grains, there is no "one experiment fits all" for non-SD grains. Experiments can be tailored to give better data, if enough information on the magnetic properties is available.

Acknowledgments
This study was carried out by Emma Hodgson as part of a Natural Environment Research Council (NERC) studentship tied to NERC grant NE/1013873/1 to Mimi J. Hill. J. Michael Grappone acknowledges support from the Duncan Norman Research Scholarship, the University of Liverpool match-funded studentship, and the NERC EAO Doctoral Training Partnership, grant NE/L002469/1. Andrew J. Biggin acknowledges support from Nederlandse Organisatie voor Wetenschappelijk Onderzoek (NWO) and a NERC Advanced Fellowship (NE/F015208/1). We thank Valera Shcherbakov and Mike Jackson for reviewing the paper and providing extensive, constructive feedback. All data will be available at the National Geological Data Centre: https://doi.org/10.5285/8e0f07ce-d8ef-4286-92bd-9019875df5cb

References

Aitken, M. J., Allsop, A. L., Bussell, G. D., & Winter, M. B. (1988). Determination of the intensity of the Earths magnetic-field during archaeological times-reliability of the Thellier technique. *Reviews of Geophysics*, *26*(1), 3–12.

Almeida, T. P., Muxworthy, A. R., Kovacs, A., Williams, W., Nagy, L., Conbhui, P. O., et al. (2016). Direct observation of the thermal demagnetization of magnetic vortex structures in nonideal magnetite recorders. *Geophysical Research Letters*, *43*, 8426–8434. https://doi.org/10.1002/2016GL070074

Biggin, A. J. (2006). First-order symmetry of weak-field partial thermoremanence in multi-domain (MD) ferromagnetic grains: 2. Implications for Thellier-type palaeointensity determination. *Earth and Planetary Science Letters*, *245*(1–2), 454–470.

Biggin, A. J. (2010). Are systematic differences between thermal and microwave Thellier-type palaeointensity estimates a consequence of multidomain bias in the thermal results? (vol 180, pg 16, 2010). *Physics of the Earth and Planetary Interiors*, *182*(3–4), 199–199.

Biggin, A. J., Badejo, S., Hodgson, E., Muxworthy, A. R., Shaw, J., & Dekkers, M. J. (2013). The effect of cooling rate on the intensity of thermoremanent magnetization (TRM) acquired by assemblages of pseudo-single domain, multidomain and interacting single-domain grains. *Geophysical Journal International*, *193*(3), 1239–1249.

Biggin, A. J., & Bohnel, H. N. (2003). A method to reduce the curvature of Arai plots produced during Thellier palaeointensity experiments performed on multidomain grains. *Geophysical Journal International*, *155*(3), F13–F19.

Biggin, A. J., & Poidras, T. (2006). First-order symmetry of weak-field partial thermoremanence in multi-domain ferromagnetic grains. 1. Experimental evidence and physical implications. *Earth and Planetary Science Letters*, *245*(1–2), 438–453.

Biggin, A. J., & Thomas, D. N. (2003a). Analysis of long-term variations in the geomagnetic poloidal field intensity and evaluation of their relationship with global geodynamics. *Geophysical Journal International*, *152*(2), 392–415.

Biggin, A. J., & Thomas, D. N. (2003b). The application of acceptance criteria to results of Thellier palaeointensity experiments performed on samples with pseudo-single-domain-like characteristics. *Physics of the Earth and Planetary Interiors*, *138*(3–4), 279–287.

Bowles, J. A., Gee, J. S., Jackson, M. J., & Avery, M. S. (2015). Geomagnetic paleointensity in historical pyroclastic density currents: Testing the effects of emplacement temperature and postemplacement alteration. *Geochemistry, Geophysics, Geosystems*, *16*, 3607–3625. https://doi.org/10.1002/2015GC005910

Bowles, J. A., & Jackson, M. J. (2016). Effects of titanomagnetite reordering processes on thermal demagnetization and paleointensity experiments. *Geochemistry, Geophysics, Geosystems*, *17*, 4848–4858. https://doi.org/10.1002/2016GC006607

Calvo, M., Prevot, M., Perrin, M., & Riisager, J. (2002). Investigating the reasons for the failure of palaeointensity experiments: A study on historical lava flows from Mt. Etna (Italy). *Geophysical Journal International*, *149*(1), 44–63.

Cisowski, S. (1981). Interacting vs non-interacting single domain behavior in natural and synthetic samples. *Physics of the Earth and Planetary Interiors*, *26*(1–2), 56–62.

Coe, R. S. (1967). Determination of paleo-intensities of Earths magnetic field with emphasis on mechanisms which could cause non-ideal behavior in Thelliers method. *Journal of Geomagnetism and Geoelectricity*, *19*(3), 157.

Coe, R. S., Riisager, J., Plenier, G., Leonhardt, R., & Krasa, D. (2004). Multidomain behavior during Thellier paleointensity experiments: Results from the 1915 Mt. Lassen flow. *Physics of the Earth and Planetary Interiors*, *147*(2–3), 141–153.

Davis, P. M., & Evans, M. E. (1976). Interacting single-domain properties of magnetite intergrowths. *Journal of Geophysical Research*, *81*(5), 989–994.

Day, R., Fuller, M., & Schmidt, V. A. (1977). Hysteresis properties of titanomagnetites—Grain-size and compositional dependence. *Physics of the Earth and Planetary Interiors*, *13*(4), 260–267.

Dunlop, D. J. (2002). Theory and application of the Day plot (M-rs/M-s versus H-cr/H-c) 1. Theoretical curves and tests using titanomagnetite data. *Journal of Geophysical Research*, *107*(B3). https://doi.org/10.1029/2001JB000486

Dunlop, D. J. (2009). Continuous and stepwise thermal demagnetization: Are they equivalent? *Geophysical Journal International*, *177*(3), 949–957.

Dunlop, D. J., & Ozdemir, O. (2001). Beyond Neel's theories: Thermal demagnetization of narrow-band partial thermoremanent magnetizations. *Physics of the Earth and Planetary Interiors*, *126*(1–2), 43–57.

Dunlop, D. J., Zhang, B. X., & Ozdemir, O. (2005). Linear and nonlinear Thellier paleointensity behavior of natural minerals. *Journal of Geophysical Research*, *110*, B01103. https://doi.org/10.1029/2004JB003095

Evans, M. E., Krasa, D., Williams, W., & Winklhofer, M. (2006). Magnetostatic interactions in a natural magnetite-ulvospinel system. *Journal of Geophysical Research*, *111*, B12S16. https://doi.org/10.1029/2006JB004454

Fabian, K. (2001). A theoretical treatment of paleointensity determination experiments on rocks containing pseudo-single or multi domain magnetic particles. *Earth and Planetary Science Letters*, *188*(1–2), 45–58.

Fabian, K., & Leonhardt, R. (2010). Multiple-specimen absolute paleointensity determination: An optimal protocol including pTRM normalization, domain-state correction, and alteration test. *Earth and Planetary Science Letters*, *297*(1–2), 84–94.

Fabian, K., & Shcherbakov, V. P. (2004). Domain state stabilization by iterated thermal magnetization processes. *Geophysical Journal International*, *159*(2), 486–494.

Haggerty, S. E. (1976). Opague mineral oxides in terrestrial igneous rocks. In Rumble, D. III (Ed.), *Reviews in mineralogy: Oxide minerals* (Vol. 3, pp. 101–300). Washington, DC: Mineralogical Society of America.
Harrison, R. J., & Feinberg, J. M. (2008). FORCinel: An improved algorithm for calculating first-order reversal curve distributions using locally weighted regression smoothing. *Geochemistry, Geophysics, Geosystems*, *9*, Q05016. https://doi.org/10.1029/2008GC001987
Hartstra, R. L. (1982a). Grain-size dependence of initial susceptibility and saturation magnetization-related parameters of four natural magnetites in the PSD-MD range. *Geophysical Journal of the Royal Astronomical Society*, *71*(2), 477–495.
Hartstra, R. L. (1982b). High-temperature characteristics of a natural titanomagnetite. *Geophysical Journal of the Royal Astronomical Society*, *71*(2), 455–476.
Hartstra, R. L. (1983). TRM, ARM and Isr of two natural magnetites of MD and PSD grain size. *Geophysical Journal of the Royal Astronomical Society*, *73*(3), 719–737.
Hill, M. J., & Shaw, J. (2000). Magnetic field intensity study of the 1960 Kilauea lava flow, Hawaii, using the microwave palaeointensity technique. *Geophysical Journal International*, *142*(2), 487–504.
Kosterov, A. A., & Prevot, M. (1998). Possible mechanisms causing failure of Thellier palaeointensity experiments in some basalts. *Geophysical Journal International*, *134*(2), 554–572.
Leonhardt, R., Heunemann, C., & Krása, D. (2004). Analyzing absolute paleointensity determinations: Acceptance criteria and the software ThellierTool4.0. *Geochemistry, Geophysics, Geosystems*, *5*, Q12016. https://doi.org/10.1029/2004GC000807
Leonhardt, R., Krasa, D., & Coe, R. S. (2004). Multidomain behavior during Thellier paleointensity experiments: A phenomenological model. *Physics of the Earth and Planetary Interiors*, *147*(2–3), 127–140.
McClelland, E., Muxworthy, A. R., & Thomas, R. M. (1996). Magnetic properties of the stable fraction of remanence in large multidomain (MD) magnetite grains: Single-domain or MD? *Geophysical Research Letters*, *23*(20), 2831–2834.
McClelland, E., & Sugiura, N. (1987). A kinematic model of TRM acquisition in multidomain magnetite. *Physics of the Earth and Planetary Interiors*, *46*(1–3), 9–23.
Muxworthy, A. R. (2010). Revisiting a domain-state independent method of palaeointensity determination. *Physics of the Earth and Planetary Interiors*, *179*(1–2), 21–31.
Muxworthy, A. R., Krasa, D., Williams, W., & Almeida, T. P. (2014). Paleomagnetic recording fidelity of nonideal magnetic systems. *Geochemistry, Geophysics, Geosystems*, *15*, 2254–2261. https://doi.org/10.1002/2014GC005249
Nagata, T., Momose, K., & Arai, Y. (1963). Secular variation of geomagnetic total force during last 5000 years. *Journal of Geophysical Research*, *68*(18), 5277.
Paterson, G. A. (2011). A simple test for the presence of multidomain behavior during paleointensity experiments. *Journal of Geophysical Research*, *116*, B10104. https://doi.org/10.1029/2011JB008369
Paterson, G. A., Biggin, A. J., Hodgson, E., & Hill, M. J. (2015). Thellier-type paleointensity data from multidomain specimens. *Physics of the Earth and Planetary Interiors*, *245*, 117–133.
Paterson, G. A., Tauxe, L., Biggin, A. J., Shaar, R., & Jonestrask, L. C. (2014). On improving the selection of Thellier-type paleointensity data. *Geochemistry, Geophysics, Geosystems*, *15*, 1180–1192. https://doi.org/10.1002/2013GC005135
Prévot, M., Lecaille, A., & Mankinen, E. A. (1981). Magnetic effects of maghemitization of oceanic crust. *Journal of Geophysical Research*, *86*(B5), 4009–4020.
Riisager, J., Perrin, M., Riisager, P., & Vandamme, D. (2001). Palaeomagnetic results and palaeointensity of Late Cretaceous Madagascan basalt. *Journal of African Earth Sciences*, *32*(3), 503–518.
Riisager, P., & Riisager, J. (2001). Detecting multidomain magnetic grains in Thellier palaeointensity experiments. *Physics of the Earth and Planetary Interiors*, *125*(1–4), 111–117.
Shaw, J. (1974). Method of determining magnitude of paleomagnetic field application to 5 historic lavas and 5 archeological samples. *Geophysical Journal of the Royal Astronomical Society*, *39*(1), 133–141.
Shcherbakov, V. P., & Shcherbakova, V. V. (2001). On the suitability of the Thellier method of palaeointensity determinations on pseudo-single-domain and multidomain grains. *Geophysical Journal International*, *146*(1), 20–30.
Shcherbakova, V. V., Shcherbakov, V. P., & Heider, F. (2000). Properties of partial thermoremanent magnetization in pseudosingle domain and multidomain magnetite grains. *Journal of Geophysical Research*, *105*(B1), 767–781.
Shcherbakov, V. P., Shcherbakova, V. V., Vinogradov, Y. K., & Heider, F. (2001). Thermal stability of pTRMs created from different magnetic states. *Physics of the Earth and Planetary Interiors*, *126*(1–2), 59–73.
Shcherbakova, V. V., Shcherbakov, V. P., Zhidkov, G. V., & Lubnina, N. V. (2014). Palaeointensity determinations on rocks from Palaeoproterozoic dykes from the Kaapvaal Craton (South Africa). *Geophysical Journal International*, *197*(3), 1371–1381.
Smirnov, A. V., Kulakov, E. V., Foucher, M. S., & Bristol, K. E. (2017). Intrinsic paleointensity bias and the long-term history of the geodynamo. *Science Advances*, *3*(2), e1602306.
Tauxe, L., & Staudigel, H. (2004). Strength of the geomagnetic field in the Cretaceous Normal Superchron: New data from submarine basaltic glass of the Troodos Ophiolite. *Geochemistry, Geophysics, Geosystems*, *5*, Q02H06. https://doi.org/10.1029/2003GC000635
Thellier, E. (1938). Sur l'aimantation des terres cuites et ses applications géophysique. *Annales de l'Institut de physique du globe de l'Université de Paris*, *16*, 157–302.
Thellier, E., & Thellier, O. (1959). Sur l'intensité du champ magnétique terrestre dans la passé historique et géologique. *Annales Geophysicae*, *6*(4), 216–376.
Wilson, R. L. (1961). Palaeomagnetism in Northern Ireland. 1. The thermal demagnetization of natural magnetic moments in rocks. *Geophysical Journal of the Royal Astronomical Society*, *5*(1), 45–58.
Xu, S., & Dunlop, D. J. (2004). Thellier paleointensity theory and experiments for multidomain grains. *Journal of Geophysical Research*, *109*, B07103. https://doi.org/10.1029/2004JB003024
Yu, Y., & Tauxe, L. (2006). Effect of multi-cycle heat treatment and pre-history dependence on partial thermoremanence (pTRM) and pTRM tails. *Physics of the Earth and Planetary Interiors*, *157*(3–4), 196–207.